Proceedings World Geothermal Congress 2015
Melbourne, Australia, 19-25 April 2015

Optimization of Silica Chemical Inhibition Using Phosphinocarboxylic Acid Copolymer through Nanocolloidal Particle Size Measurement of Simulated Geothermal Fluid

Richard C. de Guzman, Al Christopher C. de Leon, Brylee David B. Tiu, Jennifer C. Espartero, Almario D. Baltazar Jr., Rigoberto C. Advincula

Mailing address, Energy Development Corporation, One Corporate Center, Ortigas Center, Pasig City, Philippines 1605

E-mail address, deguzman.rc@energy.com.ph

Keywords: chemical inhibition, particle size, optimization, scaling, silica

ABSTRACT

Chemical inhibition is a primary preventive option to minimize silica scaling in geothermal wells and pipe lines. Effective application of inhibitors has been discussed in several studies, but the mechanism and/or action on the fluid have not been thoroughly classified. Field testing thru pilot or actual set-up is the primary conclusive test of effectivity, done by measurement of molybdate-reactive silica levels, and/or calculation of deposition rate after actual inspection. Several field studies in the Energy Development Corporation (EDC) affirmed the capability of a chemical inhibitor, phosphinocarboxylic acid copolymer, in terms of suppressing the deposition rate of silica scale in both high and low temperature application. Advanced particle size evaluation thru the use of atomic force microscopy (AFM), and dynamic light scattering (DLS) were appended to identify the optimal dosage of the phosphinocarboxylic acid inhibitor in addition to standard silicomolybdate analysis on a simulated geothermal fluid at the laboratory scale. Electrokinetic potentials were also measured for all samples. All tests were conducted at room temperature. Simulated brine with a silica saturation index (SSI) of 2.0 was used; and similar brine with an additional dose of 10ppm ferric ions to account for pipeline corrosion was also used. Overall, the results showed that 10ppm inhibitor dose appeared to be the best dosing option compared to lower doses of 5ppm and 8ppm, consistent with pilot test results previously conducted.

1. INTRODUCTION

Extensive studies have been conducted with regard to silica science as part of colloidal chemistry and as part of scaling studies. Silica is one of the most abundant elements in the earth's crust and thus is expected to occur naturally and in different forms in the geological formations. The presence of silica in geothermal fluid is one of the major considerations in designing operational conditions and effectively, the amount of heat harnessed from the fluid itself as discussed by Fournier (1979), Gunnarson et al (2003) and Angcoy (2006). In extreme cases of significantly high silica levels, the fluid may not be used unless there are mitigating measures outweighing the possibility of massive scaling in the wells and/or pipelines. Silica levels are currently monitored using the silica saturation index (SSI), which like any other saturation indices, is a ratio of the fluid's silica content over the equilibrium silica that can be dissolved at a given temperature. The equilibrium silica levels are estimated by an empirical model by Fournier (1979) and further refined by chloride correction by Fournier and Potter (1982). This study looks further into the nanocolloidal silica scaling formation using new characterization techniques such as the atomic force microscope (AFM) to evaluate the extent of a chemical inhibitor's action on the nanocolloidal formation.

The mechanism of formation is expected to be more of a colloidal than a monomeric deposition process, and this is summarized in Figure 1 by Bergna and Roberts (2006). Colloidal deposition occurs via a condensation polymerization step forming small molecular weight dimers and trimers prior to the forming of rings of various sizes and cross-linked polymeric chains to complex and amorphous product as discussed by Amjad (2010). In contrast, monomeric or direct deposition relies on the interaction of the metal to single silica groups, or monomers. Sinclair (2012) discusses that this process usually occurs at basic conditions (pH>8).

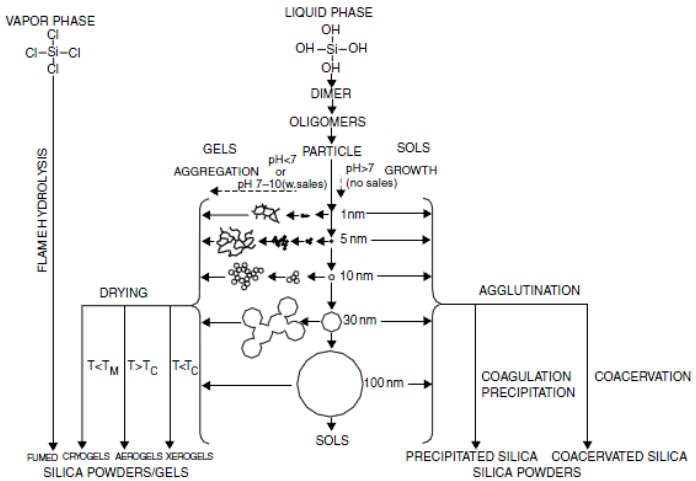

Figure 1: Condensation polymerization pathways from monomeric silica by Bergna and Roberts (2006).

Energy Development Corporation (EDC) has used chemical inhibition as its primary mitigating measure for scaling fluids. This is on top of operational exigencies, particularly the management of separation and line pressures which are a part of standard protocol. Baltazar et al (1997) found out the effectivity of phophino-carboxylic acid copolymer for ultra-high silica levels, and similarly, de Guzman et al (2013) tested the same inhibitor for a low-temperature medium-term discharge set-up. Effectiveness of such inhibitors have been confirmed on laboratory, pilot and actual field tests but the microscopic-level mechanism of inhibition has not been investigated extensively and is not yet fully understood.

In the study of Baltazar et al (1997), three inhibitor concentrations were tested at 5.0, 8.0, and 10.0 ppm. The average efficiency results were based on the silica inhibitor level as seen in Table 1.

Table 1: Pilot side test results using phosphinocarboxylic acid copolymer as inhibitor by Baltazar et al (1997).

Inhibitor Concentration	Average Efficiency, %
5.0 ppm	38
8.0 ppm	35
10.0 ppm	96

In this study, the new methods of characterization/reference by looking at the nanocolloidal silica formation were used to optimize the inhibitor dosing. Standard silicomolybdate tests were also used as baseline data for the optimization study. It has been reported that underdosing and overdosing could induce scaling of the fluid, and to assure an efficient and effective dosing set-up would translate to good economic returns.

2. EXPERIMENTAL DESIGN

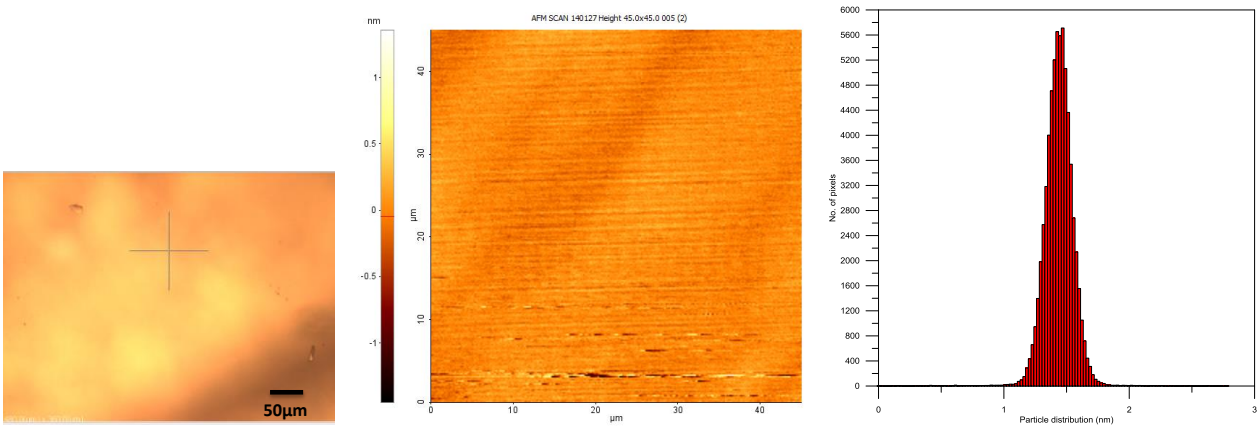

(a) **(b)** **(c)**

Figure 2: Fresh mica surface scans using different methods using (a) optical microscopy, and from AFM scan (b) topography image and (c) height distribution.

The silica solutions were prepared from $Na_2SiO_2 \bullet 5H_2O$, which was passed through cation exchange resins and kept in plastic containers while in another container, the rest of the brine was prepared from reagent-grade salts. The two solutions were mixed to achieve the target brine chemistry and was pH-corrected to neutral levels (7.0-7.5) identified as the zone of minimum silicic acid solubility as discussed by Amjad (2010). The final chemistry is based on one of the actual wells except that the final SSI was maintained at just 2.0. In addition, different inhibitor treatments were used in the samples which were identified at 5.0ppm, 8.0ppm and 10.0 ppm. This study uses the same inhibitor tested by Baltazar (1997) in the Botong sector.

Several tests, including the conventional molybdate-reactive silica concentration tests (guided by ASTM D859-00), particle size measurement tests (atomic force microscopy or AFM, dynamic light scattering or DLS and transmission electron microscopy or TEM) and zeta potential meter, were used.

For silica deposited on a solid substrate, mica was used in testing using the AFM.

3. RESULTS AND DISCUSSION

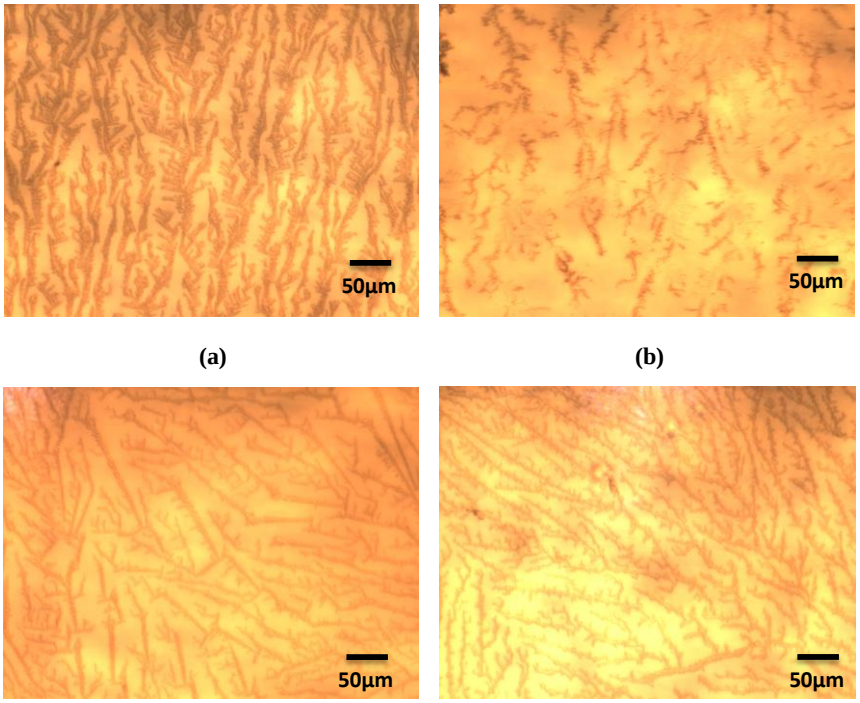

(a) **(b)**

(c) **(d)**

Figure 3: Optical images of tested brine (no iron content) with SSI 2.0 for (a) untreated treated samples (b) 5.0ppm (c) 8.0 ppm and (d) 10.0 ppm of inhibitor.

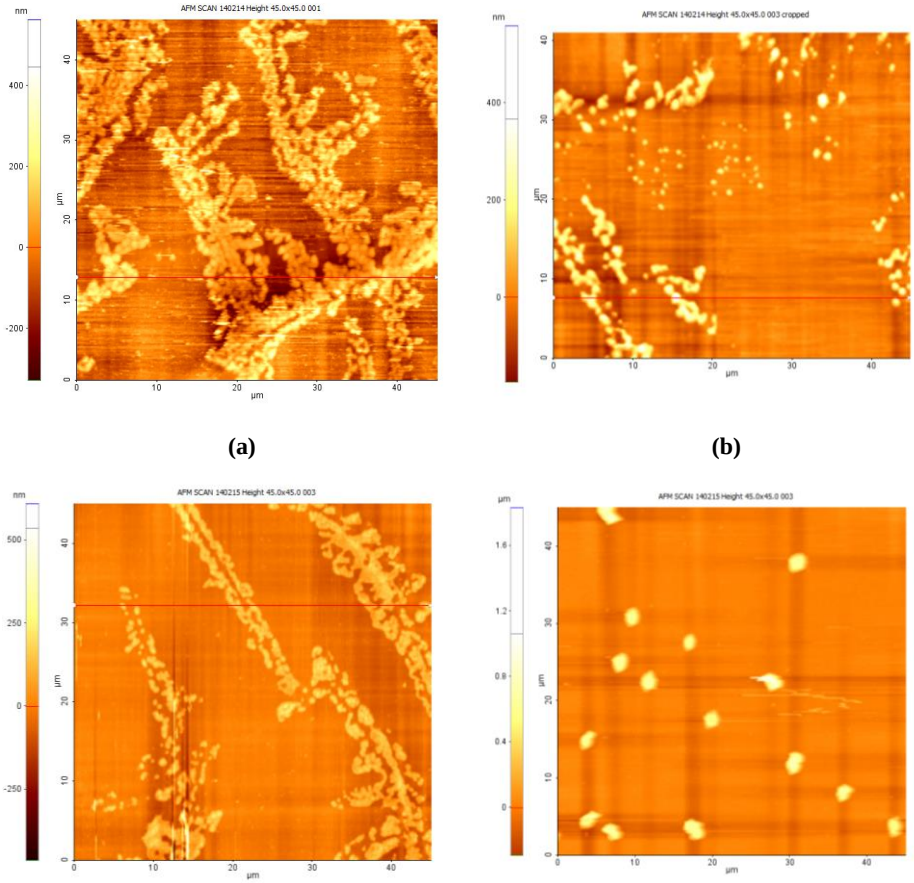

(a) **(b)**

(c) **(d)**

Figure 4: AFM images of tested brine (no iron content) with SSI 2.0 for (a) untreated treated samples (b) 5.0ppm (c) 8.0 ppm and (d) 10.0 ppm of inhibitor.

For a clear baseline, blank or freshly exfoliated mica substrates were imaged using the optical microscope and the AFM shown in Figure 2. These show a clean surface with height profiles almost negligible. Height profiles manifested by the histogram of the number of pixels per measured levels was standardized and used to provide a measure of the most dominant height levels of the silica nanoparticles on the substrate. From these scans, mica manifested a height distribution of 1-2 nm. These height levels are negligible compared to the sample scans obtained.

The first set of images in Figure 3 and 4 includes the simulated brine with no iron content, untreated and treated at different levels.

The optical images capture the book definition of the formation of the silica nanoparticles which is shown in Figure 5. Iler (1979) describes it as the natural order of formation of polymeric silica and is consistent with the condensation polymerization mechanism. It is very interesting that upon settling from the solution and in increasing inhibitor dosing, the treated samples tend to move closer to what the untreated sample appears to be. This, however, is not the same case for the AFM scans where the 10ppm-dosed samples formed larger particles already and these mask the smaller particles in solution. A more accurate way of seeing this trend is by looking at the silicomolybdate tests, the AFM height profiles and the DLS particle distribution in Figure 6.

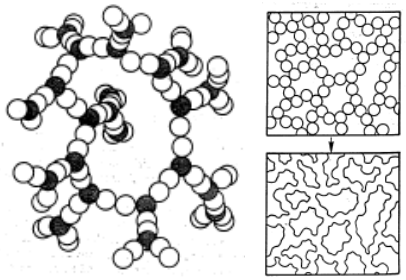

Figure 5: Silica colloid formation visual description from Iler (1979).

Several treatments led to sizes which are beyond the limit of oligomer formation, like in Figure 4d where the heights were able to reach as high as 1600nm. At this point, these heights correlate to a point where the particles have already managed to attain a coagulated state. Figure 6c is a plot of the results of the DLS scan, this presents the percent mass distribution in the y-axis of the various reported hydrodynamic radii of particles in the solution (visualized and labeled in plot, noted above particle).

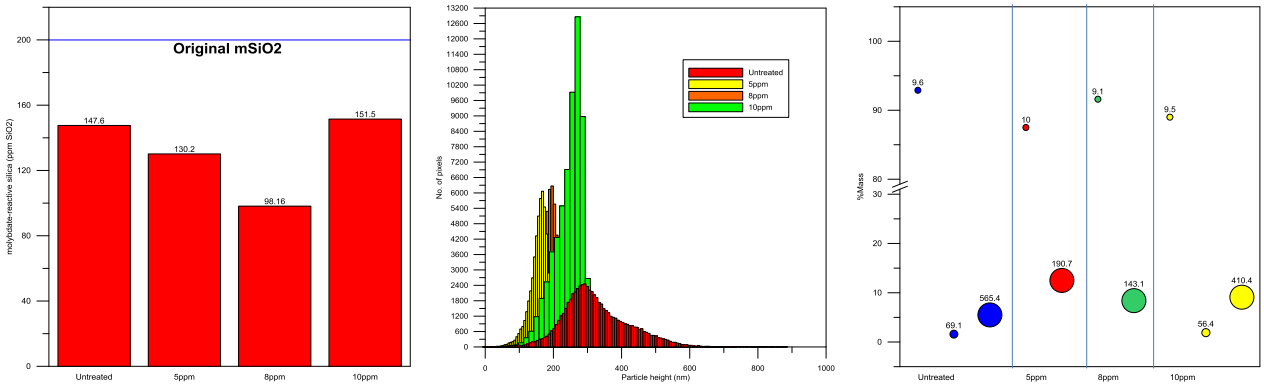

(a) **(b)** **(c)**

Figure 6: (a) Oligomeric silica levels measured by colorimetric methods, (b) particle height distribution from AFM scans and (c) DLS particle size distribution profiles.

Oligomeric silica levels clearly indicate that the 10ppm is the one that is effective, with the lower order of dose actually even decreasing the molybdate-reactive silica to be less than the untreated, an indication that it induces scaling but more tests are ought to be conducted to be able to confirm this. In terms of the particles' size upon settling to a surface and in solution using the AFM and DLS respectively, it is indeed confirmed that as the dose increases, the closer the particle size in surface is to that of the untreated sample. While in solution, there is a certain split grouping the silica particles from two (small and big) to three including an intermediary size.

On the other hand, the same brine samples were tested with an addition of 10ppm iron. The extensive supply was used to assume a case of corroding pipelines and its effect to the nanoscale formation and the particle size distribution. The AFM scans are presented in Figure 7. Similar to Figure 4d, Figure 7a reports extremely high heights at 1200nm, again representing a state of coagulation among the particles, beyond an oligomeric formation state.

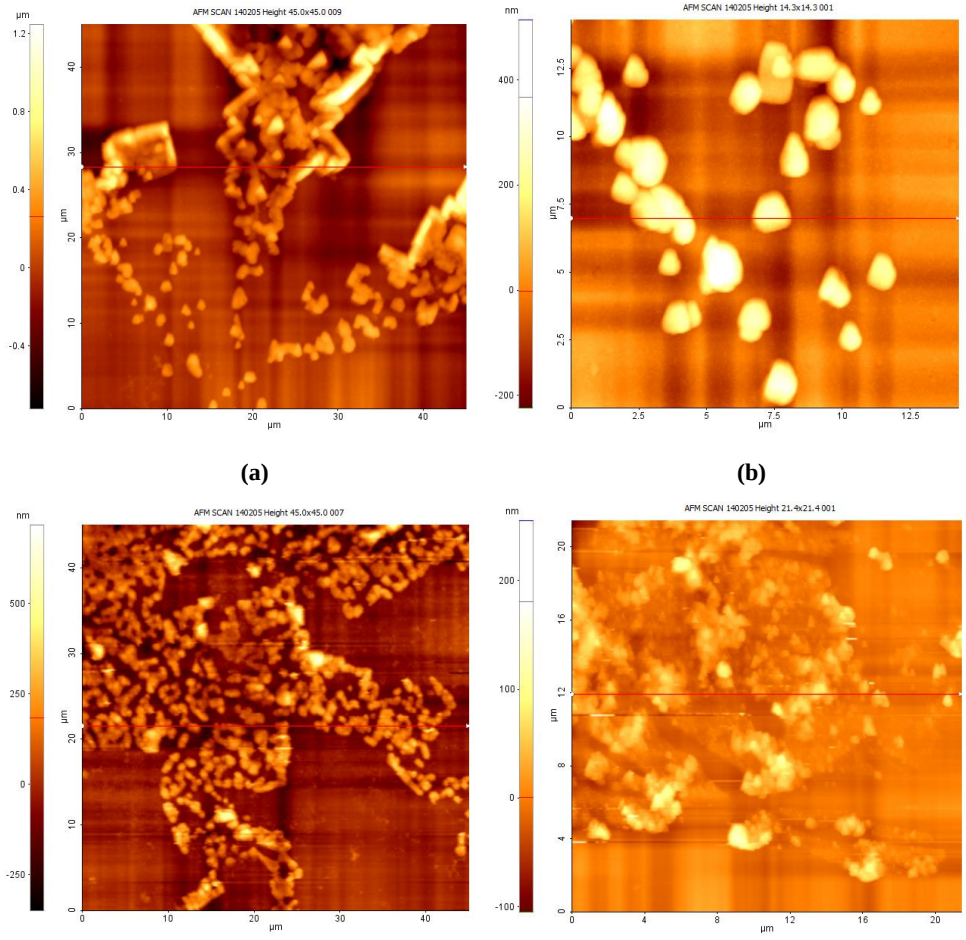

Figure 7: AFM images of tested brine (10ppm iron content) with SSI 2.0 for (a) untreated treated samples (b) 5.0ppm (c) 8.0ppm and (d) 10.0ppm.

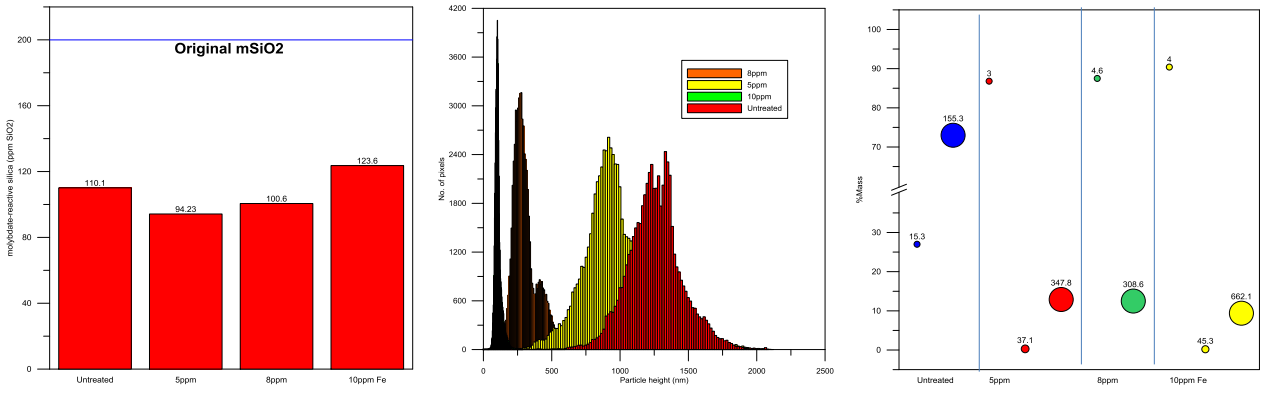

Figure 8: (a) Oligomeric silica levels measured by colorimetric methods, (b) particle height distribution from AFM scans and (c) DLS particle size distribution profiles.

One major difference between the two sets of AFM images is that this time, with the presence of Fe in the brine, the formation of distinct spherical particles are no longer obvious. This is a significant step away from that of the former set-up with no ferric ions at all. A coagulating effect may have caused this phenomenon, and the particle sizes were also compared in Figure 8. In terms of the silicomolybdate test, the 10ppm dose is still the one effective dosing level of the three and similarly, the lower doses have lower silica levels compared to that of the untreated samples. The major deviation here is based on the particle height profile of the settled

oligomers with a very distinct shift in peak height from the untreated to that of the 10ppm-dosed samples. In addition, the untreated sample in solution already has large particles to begin with compared to the rest as shown in the DLS scans.

Phosphinocarboxylic acid copolymer inhibitor most probably behaved similarly as the other anionic inhibitors, with inhibition mechanism similar to that of Figure 9 by Demadis et al (2011). Anionic inhibitors are believed to act on the seeding nucleus.

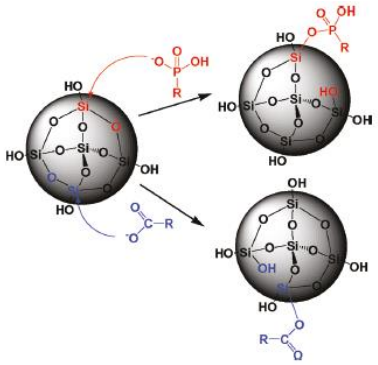

Figure 9: Silica inhibition mechanisms anionic polymers by Demadis et al (2011).

Another method of evaluation tests was the measurement of the solution's zeta potential. For colloidal formations, this is similar to the charge of an ion. Silica colloids are expected to have a negative zeta potential but these were not measured here probably because of the presence of several other ions in the solution. In Figure 10a, upon reaching a 10ppm dose, a negative zeta potential value was observed (possibly a good correlation with that of the silicomolybdate test) while for Figure 10b, the zeta potential was still increasing.

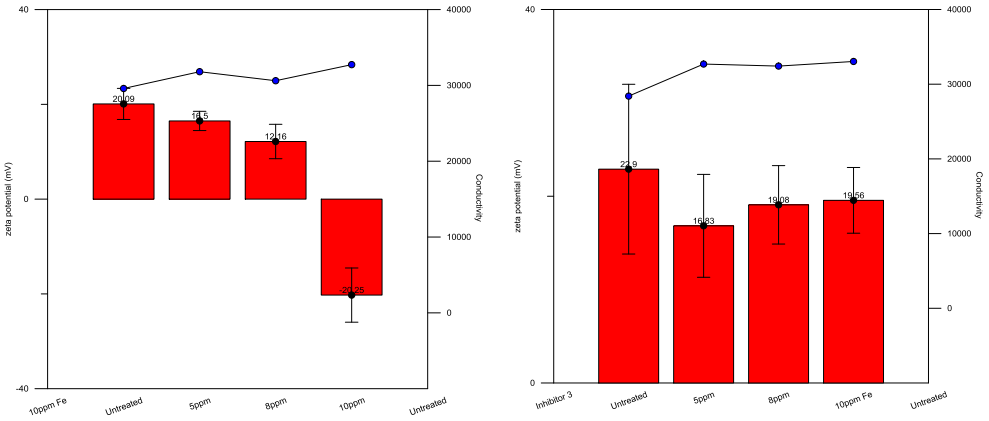

(a) **(b)**

Figure 10: Zeta potential and conductivity measurements for simulated brine with (a) no Fe and (b) 10ppm Fe.

4. CONCLUSION AND RECOMMENDATIONS

For chemical inhibition techniques, to optimize the dose and set-up is an important way to ensure practical and economical use of resources. New methods of testing were used to determine the optimum dose of a phosphinocarboxylic acid copolymer inhibitor in laboratory conditions, and the same methods are to be evaluated for actual field testing and application. In addition to the standard silicomolybdate testing, the samples were also tested using particle height measurements upon settling via atomic force microscopy (AFM), particle's hydrodynamic radius in solution via dynamic light scattering (DLS) and electrokinetic or zeta potentials. In addition, an excessive supply of ferric ions was added to another set to evaluate the effect of already corroded lines in scaling. Based on the silicomolybdate levels, there is an improved increase in the silica concentration level and this is consistent with the DLS results with a sharp drop in the mass percent of the oligomeric silica level. In the AFM scans, there is an apparent increase in the linking among the particles on the mica surface. There is a distinct difference measured here between the silicomolybdate levels with no and with 10ppm iron which is consistent with previous studies.

Of the three levels of dose at the tested conditions, the 10ppm dosing still appeared to be the most effective. This is consistent with the results of Baltazar et al (1997). The degree of aggregation of the different treatments was distinguishable from the scans gathered especially with the high iron content brine.

Zeta potentials on the other hand was capable of showing a declining trend for the simulated geothermal brine, and was even able to reach negative values at levels of efficient application.

ACKNOWLEDGEMENTS

We gratefully acknowledge the technical support from Dr. E. Karathanasis and group from the Biomedical Engineering Department, Dr. S. Rowan and group, Katrina Pangilinan and Joey Mangadlao of the Macromolecular Science and Engineering Department and the School of Medicine of Case Western Reserve University and Park Systems.

REFERENCES

Amjad, Z.: The Science and Technology of Industrial Water Treatment, Boca Raton, Florida: *Taylor & Francis Group*, LLC (2010).

Angcoy, E.: An Experiment on Monomeric and Polymeric Silica Precipitation Rates from Supersaturated Solution, *Geothermal Training Programme*, The United Nations University, **5**, (2006).

Baltazar, A., Garcia, S., Solis, R., and Jordan, O.: Silica Scale Inhibition Experiments: Geogard SX Application on Geothermal Brine With Ultra High Concentration of SiO_2, *Meeting the Challenge of Increased Competition*, Geothermal Resources Council, (1997), 43-48.

Bergna, H., and Roberts W.: Colloidal Silica: Fundamentals and Applications, Boca Raton, Florida: *CRC Press*, (2006).

Brown, K.: Thermodynamics and kinetics of silica scaling, *International Workshop on Mineral Scaling*, Manila, (2011).

de Guzman, R., See, F., Baltazar, A., and Salonga, N.: Silica Scale Inhibition by Phosphino-carboxylic Acid Copolymer in Low-temperature Injection of Geothermal Fluid, Tagaytay City, Philippines: Asian Geothermal Symposium, (2013).

Demadis, K., Somara, M. and Mavredaki, E.: Additive-Driven Dissolution Enhancement of Colloidal Silica, 1. Basic Principles and Relevance to Water Treatment, *Industrial and Engineering Chemistry Research*, (2011), 12587-12595.

Fournier, R.: The solubility of amorphous silica in water at high temperatures and high pressures, *American Mineralogist*, **62**, (1977), 1052-1056.

Fournier, R. and Potter, R.: A revised and expanded silica (quartz) geothermometer, *Geothermal Resources Council*, **11-10**, (1982).

Gunnarson, I. and Arnorsson S.: Silica scaling: The main obstacle in efficient use of high-temperature geothermal fluids, *International Geothermal Conference*, (2003), 30-36.

Sinclair, L.: Development of a Silica Scaling Test Rig, University of Canterbury, 2012.